

Published in final edited form as:

*Hepatology*. 2015 March ; 61(3): 930–941. doi:10.1002/hep.27492.

## Axl Activates Autocrine Transforming Growth Factor- $\beta$ Signaling in Hepatocellular Carcinoma

Patrick Reichl<sup>1</sup>, Mirko Dengler<sup>1</sup>, Franziska van Zijl<sup>1</sup>, Heidemarie Huber<sup>1</sup>, Gerhard Führlinger<sup>1</sup>, Christian Reichel<sup>2</sup>, Wolfgang Sieghart<sup>3</sup>, Markus Peck-Radosavljevic<sup>3</sup>, Markus Grubinger<sup>1</sup>, and Wolfgang Mikulits<sup>1</sup>

<sup>1</sup>Department of Medicine I, Division: Institute of Cancer Research, Comprehensive Cancer Center, Medical University of Vienna, Vienna, Austria

<sup>2</sup>AIT Seibersdorf Laboratories, Seibersdorf, Austria

<sup>3</sup>Department of Internal Medicine III, Division of Gastroenterology and Hepatology, Medical University of Vienna, Vienna, Austria.

### Abstract

In hepatocellular carcinoma (HCC), intrahepatic metastasis frequently correlates with epithelial to mesenchymal transition (EMT) of malignant hepatocytes. Several mechanisms have been identified to be essentially involved in hepatocellular EMT, among them transforming growth factor (TGF)- $\beta$  signaling. Here we show the up-regulation and activation of the receptor tyrosine kinase Axl in EMT-transformed hepatoma cells. Knockdown of Axl expression resulted in abrogation of invasive and transendothelial migratory abilities of mesenchymal HCC cells *in vitro* and Axl overexpression-induced metastatic colonization of epithelial hepatoma cells *in vivo*. Importantly, Axl knockdown severely impaired resistance to TGF- $\beta$ -mediated growth inhibition. Analysis of the Axl interactome revealed binding of Axl to 14-3-3 $\zeta$ , which is essentially required for Axl-mediated cell invasion, transendothelial migration, and resistance against TGF- $\beta$ . Axl/14-3-3 $\zeta$  signaling caused phosphorylation of Smad3 linker region (Smad3L) at Ser213, resulting in the up-regulation of tumor-progressive TGF- $\beta$  target genes such as PAI1, MMP9, and Snail as well as augmented TGF- $\beta$ 1 secretion in mesenchymal HCC cells. Accordingly, high Axl expression in HCC patient samples correlated with elevated vessel invasion of HCC cells, higher risk of tumor recurrence after liver transplantation, strong phosphorylation of Smad3L, and lower survival. In addition, elevated expression of both Axl and 14-3-3 $\zeta$  showed strongly reduced survival of HCC patients.

**Conclusion**—Our data suggest that Axl/14-3-3 $\zeta$  signaling is central for TGF- $\beta$ -mediated HCC progression and a promising target for HCC therapy.

---

Copyright © 2014 by the American Association for the Study of Liver Diseases.

Address reprint requests to: Wolfgang Mikulits, Ph.D., Department of Medicine I, Division: Institute of Cancer Research, Comprehensive Cancer Center, Medical University of Vienna, Borschke-Gasse 8A, 1090 Vienna, Austria. wolfgang.mikulits@meduniwien.ac.at; fax: +43 1 40160 957519.

Author names in bold designate shared co-first authorship.

Supporting Information

Additional Supporting Information may be found at [onlinelibrary.wiley.com/doi/10.1002/hep.27492/supinfo](http://onlinelibrary.wiley.com/doi/10.1002/hep.27492/supinfo).

Potential conflict of interest: Dr. Sieghart consults, advises, is on the speakers' bureau, and received grants from Bayer.

Hepatocellular carcinoma (HCC) is the fifth most prevalent cancer and accounts for ~5% of all cancer cases worldwide.<sup>1,2</sup> Major risk factors include viral infections with hepatitis B or C (HBV, HCV), exposure to aflatoxin, or alcohol intoxication. Further risk emanates from nonalcoholic fatty liver disease caused by obesity or diabetes. These factors induce hepatic inflammation and fibrosis and lead to cirrhosis, as observed in 80% of HCC cases.<sup>1</sup>

Hepatocytes show aberrant proliferation and dedifferentiation during HCC development. The underlying mechanisms are diverse and involve activation of transforming growth factor (TGF)- $\beta$  signaling, which leads to epithelial to mesenchymal transition (EMT) and enhanced cell migration.<sup>3,4</sup> Local invasion of HCC cells and intrahepatic metastasis frequently correlate with EMT. While TGF- $\beta$  acts as tumor-suppressive during healthy conditions and early tumor development, malignant hepatocytes benefit from TGF- $\beta$  signaling at advanced HCC stages by antagonizing cytostatic and cytotoxic effects and by inducing EMT.<sup>5,6</sup> Activation of canonical TGF- $\beta$  signaling is caused by binding of TGF- $\beta$  to heteromeric TGF- $\beta$  type I and II receptors, which phosphorylate Smad2 and Smad3 at the C-termini, resulting in complex formation with Smad4 and nuclear translocation to modulate gene transcription.<sup>7</sup> Phosphorylation of Smad linker regions (SmadL) that separate N-terminal Mad homology (MH)1 and C-terminal MH2 domains by mitogen activated protein kinases (MAPKs) such as extracellular signal-regulated kinase (ERK), c-Jun N-terminal kinase (JNK), and p38 MAPK is suggested to play a pivotal role in activation of TGF- $\beta$  Smad target genes.<sup>8</sup>

Malignant hepatocytes that are transdifferentiated to a mesenchymal phenotype during EMT show loss of cell-to-cell contacts, which allow escape from tumor mass by individual cell movement.<sup>9</sup> Transcriptional repressors of epithelial gene expression such as Snail, ZEB1, and ZEB2 or Twist are essentially involved in EMT and either directly or indirectly induced by signaling from TGF- $\beta$ /Smad, receptors tyrosine kinases (RTKs), integrins, Notch, Sonic Hedgehog, or Wnt/ $\beta$ -catenin.<sup>10</sup> Yet it is poorly understood how TGF- $\beta$ /Smad collaborates with RTKs to selectively induce a mesenchymal gene expression program driving tumor progression and metastasis. In HCC, both epidermal growth factor receptor (EGF-R) and Met are suggested to overcome tumor-suppressive effects of TGF- $\beta$ /Smad by escaping apoptosis and chemosensitivity.<sup>11,12</sup>

Tyro3, Axl, and Mer are RTKs of the TAM receptor family.<sup>13</sup> Overexpression of Axl correlates with poor survival of tumor patients and was detected in various types of cancer.<sup>14</sup> Activation of Axl signaling by its ligand Gas6 leads to enhanced proliferation, survival, invasion, and metastasis of cancer cells. In HCC, *in situ* hybridization revealed up-regulation of Axl and a further study suggested that Axl acts downstream of the Hippo pathway to trigger cell invasion and metastasis.<sup>15,16</sup> In breast carcinoma, autocrine activation of Axl by Gas6 is essential for EMT and metastatic dissemination<sup>17</sup> and antagonizing Axl signaling inhibits pulmonary metastasis.<sup>18</sup>

The 14-3-3 proteins belong to a family of highly conserved isoforms that bind to signal components involved in various cellular processes.<sup>19</sup> The interactions between 14-3-3 and its targets are mostly mediated by the phosphorylation of the binding protein. In HCC, overexpression of 14-3-3 $\zeta$  is frequently observed.<sup>20</sup> In addition, 14-3-3 $\zeta$  complexed in  $\alpha$ B-

crystallin induces EMT of HCC cells and overexpression of both  $\alpha$ B-crystallin and 14-3-3 $\zeta$  correlates with poor HCC survival.<sup>21</sup>

In this study we show the molecular collaboration of Axl and TGF- $\beta$ /Smad signaling upon HCC progression. Axl regulates mesenchymal gene expression in HCC cells by interaction with 14-3-3 $\zeta$  that causes aberrant phosphorylation of Smad3L and induction of tumor-progressive TGF- $\beta$  functions. Analysis of primary HCC samples supports the crucial role of Axl/14-3-3 $\zeta$  in patient survival and suggests Axl as a novel auspicious target to combat HCC progression.

## Materials and Methods

### Immunohistochemistry and Tissue Array Analysis

Xenograft tissue was fixed in 4% paraformaldehyde and embedded in paraffin. The 4- $\mu$ m sections were stained with anti-green fluorescent protein (GFP) antibody at a dilution of 1:100. To analyze Axl, 14-3-3 $\zeta$ , phospho-Smad3L, and TGF- $\beta$ 1 expression in primary HCC, tissue arrays were employed containing paraffin-embedded specimens of tumors and adjacent normal tissue collected from a total of 133 female and male HCC patients. All patients had undergone orthotopic liver transplantation for HCC at the Department of Transplantation Surgery, Medical University of Vienna, between 1982 and 2002, as described.<sup>9</sup> All histological specimens were reviewed for histological type and grade by two individual board-certified pathologists. The 4- $\mu$ m-thick sections of core biopsies arrayed in triplicate were stained with anti-Axl antibody (R&D Systems, Minneapolis, MN), anti-14-3-3 $\zeta$  antibody (Abcam, Cambridge, UK), anti-phospho-Smad3L antibody (Ser213; Abcam), or anti-TGF- $\beta$ 1 antibody (Santa Cruz Biotechnology, Santa Cruz, CA), all at a dilution of 1:100. Secondary antibody was employed and visualization was performed with the vectastain ABC kit using diaminobenzidine as substrate (Vector Laboratories, Burlingame, CA). Evaluation of tissue arrays was performed by three independent researchers (P.R., M.D., and F.v.Z.) who were blinded regarding patient details. Immunostaining for Axl, phospho-Smad3L, and TGF- $\beta$ 1 was scored by using the following arbitrary scale: no, low, medium, and high staining. Immunostaining with anti-14-3-3 $\zeta$  antibody was scored low, medium, and high staining, as no tissue showed the absence of 14-3-3 $\zeta$ .

Detailed information on experimental procedures can be found in the Supporting Material.

## Results

### Axl Is Up-Regulated and Activated in Mesenchymal HCC Cells

We assessed the expression of TAM receptors in epithelial 3p and mesenchymal 3sp hepatoma cells.<sup>22</sup> Transcriptome profiling revealed a 30.9-fold and 8.7-fold up-regulation of Axl and its ligand Gas6 in mesenchymal 3sp cells, respectively. Contrary to this, transcript levels of Mer and Tyro3 as well as their ligand protein S were reduced to 0.7-fold, 0.5-fold, and 0.05-fold, respectively (Fig. 1A). Expression of Axl was confirmed by quantitative reverse-transcription polymerase chain reaction (qRT-PCR) and immunoblotting (Fig. 1B,C). Immunofluorescence analysis showed localization of Axl at cellular membranes of

mesenchymal 3sp cells (Fig. 1D). In addition, phospho-RTK analysis displayed phosphorylation of the intracellular kinase domain of Axl in mesenchymal cells, while activation of Tyro3 and Mer was 10-fold decreased or even lost as compared to epithelial hepatoma cells, respectively (Fig. 1E,F).

### Axl Augments Cell Migration and Transendothelial Invasion

Analysis of Axl expression by enzyme-linked immunosorbent assay (ELISA) revealed high levels in the majority of mesenchymal HCC cell lines, whereas epithelial hepatoma lines were mostly devoid of Axl protein (Fig. 2A). Furthermore, Axl expression strongly correlated with an enhanced migratory phenotype in all cell lines ( $n = 14$ ; Fig. 2A; Supporting Fig. 1), suggesting a role of Axl in cell migration. Immunoprecipitation (IP) of Axl and probing with an anti-phosphotyrosine antibody revealed enhanced phosphorylation of Axl in Gas6-stimulated mesenchymal 3sp cells (Fig. 2B). Accordingly, migration of 3sp cells as well as transendothelial invasion through a layer of HSECs were 4-fold ( $P < 0.001$ ) and 3-fold ( $P < 0.001$ ) increased after stimulation with Gas6 as compared to control (3sp-siNT and 3spAxl-siNT, both without Gas6), respectively (Fig. 2C,D; Supporting Fig. 2). Knockdown of Axl in 3sp cells (Fig. 1C) reduced these effects, while overexpression of Axl significantly enhanced them 7-fold ( $P = 0.048$ ) and 3.7-fold ( $P < 0.001$ ). These data indicate a major role of Gas6/Axl signaling in individual cell movement and intravasation of mesenchymal HCC cells into blood endothelial cells.

### Interaction With 14-3-3 $\zeta$ Is Necessary for Axl-Mediated Cell Migration

Mass spectrometry analysis of Axl-IPs in 3sp cells revealed 14-3-3 $\zeta$  as an interaction partner of Axl (data not shown), which was validated by pull-down of 14-3-3 $\zeta$  and probing with anti-Axl antibody (Fig. 2B). Binding of 14-3-3 $\zeta$  to Axl was independent of Gas6 stimulation of Axl, suggesting that 14-3-3 $\zeta$  acts as an adaptor or scaffold protein of Gas6/Axl signaling rather than a modulator of Axl conformation allowing RTK phosphorylation. Interestingly, interference with 14-3-3 $\zeta$  by siRNA diminished Gas6/Axl-dependent migratory and invasive responses in mesenchymal 3sp cells as well as in 3sp cells overexpressing Axl (Fig. 2C,D), suggesting that Axl requires interaction with 14-3-3 $\zeta$  for downstream signaling.

### Axl Enhances Tumor Growth and Metastatic Potential of HCC Cells

Poorly migrating epithelial PLC/PRF/5 cells that almost lack Axl protein expression (Fig. 2A) were employed for stable overexpression (PLC-Axl;  $n = 4$ ). Xenografting of PLC-Axl cells showed increased tumor growth as compared to control PLC-GFP cells ( $n = 4$ ;  $P = 0.044$ ; Fig. 2E). To assess metastasis formation, subcutaneous tumors from PLC-GFP ( $n = 4$ ) and PLC-Axl ( $n = 4$ ) were resected and lungs were analyzed 30 days postsurgery by immunohistochemical staining of GFP (Fig. 2F). Metastatic nodules could be identified in three out of four animals with PLC-Axl tumors, whereas no pulmonary metastasis was observed in control animals. From these data we concluded that Axl drives tumor-igenesis and enhances metastatic dissemination *in vivo*.

## Axl Mediates Resistance Against TGF- $\beta$ and Regulates Effectors of TGF- $\beta$ Signaling

Proliferation of 3sp cells was monitored over 7 days. Knockdown of Axl or 14-3-3 $\zeta$  alone did not affect proliferation (Supporting Fig. 3A,B), whereas cell survival was significantly impaired in the presence of TGF- $\beta$ 1 (Fig. 3A,B;  $P < 0.001$ ) as compared to nontarget controls. To determine cell death, TdT-mediated dUTP-biotin nick end labeling (TUNEL) assays were performed with 3sp cells exposed to TGF- $\beta$ . Knockdown of Axl strongly increased susceptibility to TGF- $\beta$ -induced cell death as compared to control cells (Fig. 3C). Cell cycle analysis revealed a significant increase of cells in G1 or G2 in response to TGF- $\beta$ 1 upon interference with Axl or 14-3-3 $\zeta$  (Supporting Fig. 3C). Notably, knockdown of Axl alone did not significantly affect cell cycle, while intervention with 14-3-3 $\zeta$  augmented G1 phase, probably due to broad implications of 14-3-3 $\zeta$  in cell cycle progression. These data suggest an important role of Axl in protecting HCC cells from TGF- $\beta$  mediated cell death and cell cycle arrest, causing resistance against TGF- $\beta$  in HCC.

We next investigated the impact of Gas6/Axl on TGF- $\beta$  downstream effectors in mesenchymal 3sp cells using phospho-specific antibody microarrays. Interestingly, stimulation with Gas6 strongly increased phosphorylation of the Smad3L region (2.3-fold;  $P < 0.001$ ), in particular on Ser213 ( $P < 0.001$ ; Fig. 4A), while Ser204/208 remained unaffected. In addition, activation of the C-terminal region was observed on Ser425, although to a lesser extent ( $P < 0.001$ ). Importantly, interference with Axl or 14-3-3 $\zeta$  abolished aberrant Smad3 phosphorylation. We further observed activation of PI3K/AKT signaling at multiple levels (Fig. 4B), particularly of AKT1 (Ser246, Thr450, Tyr474;  $P < 0.001$ ) and PI3K (Tyr607, Tyr467/199;  $P < 0.001$ ), which could be verified by immunoblotting (Fig. 4C). In addition, ERK signaling remained unaffected, whereas phosphorylation of JNK was strongly enhanced (3.5-fold, Tyr185;  $P < 0.001$ ; Fig. 4B,D). These changes in phosphorylation of AKT1 and JNK were reversed after knockdown of Axl or 14-3-3 $\zeta$ . Interference with JNK abolished the increase in Smad3L phosphorylation in response to Gas6, while activation of Smad2 remained unaffected (Fig. 4D). These results suggest that Gas6/Axl/14-3-3 $\zeta$  signaling activates a multitude of TGF- $\beta$  downstream effectors involved in cell survival and TGF- $\beta$  resistance, most notably JNK leading to phosphorylation of the Smad3L region.

## Axl/14-3-3 $\zeta$ Activates Tumor-Promoting Target Genes of TGF- $\beta$

To further study the impact of Axl on TGF- $\beta$  signaling, we performed qRT-PCR of tumor-promoting TGF- $\beta$  target genes such as plasminogen activator inhibitor (PAI)1, matrix metalloproteinase (MMP)9, and Snail. TGF- $\beta$  target genes were analyzed after stimulation with Gas6 in several epithelial (PLC/PRF/5, HepG2, and 3p) and mesenchymal (HLF, SNU449, and 3sp) cell lines. Remarkably, with the exception of MMP9 in HLF cells, expression levels of target genes were strongly increased in all mesenchymal cell lines, whereas none of the epithelial cell lines showed alterations in mRNA expression in response to Gas6 (Fig. 5A-C). Most notably, knockdown of Axl or 14-3-3 $\zeta$  in 3sp cells reversed these effects almost completely, except for Snail, where a reduction was observed without statistical significance ( $P < 0.001$  for PAI1 and MMP9; Fig. 5D). A comparable decrease was observed for TGF- $\beta$ 1 after interference with Axl or 14-3-3 $\zeta$  in 3sp cells ( $P < 0.01$ ). Pharmacological inhibition of TGF- $\beta$  signaling completely reversed the promigratory and

proinvasive effects of Gas6 in 3sp cells (Supporting Fig. 4A,B). From these data we concluded that Axl/14-3-3 $\zeta$  signaling enhances expression of tumor-promoting TGF- $\beta$  target genes including TGF- $\beta$ 1, leading to an enhanced invasive phenotype of mesenchymal HCC cells.

### Axl Induces Autocrine TGF- $\beta$ Secretion

Next we analyzed TGF- $\beta$ 1 mRNA expression by qRT-PCR after stimulation with Gas6 in epithelial as well as mesenchymal hepatoma lines. Axl activation significantly increased TGF- $\beta$ 1 expression in two of three mesenchymal cell lines (SNU449 and 3sp), whereas no effect could be observed in epithelial cells (Fig. 5E). Interestingly, expression of Axl correlated with TGF- $\beta$ 1 secretion in epithelial and mesenchymal hepatoma cells ( $n = 14$ ;  $R = 0.60$ ;  $P < 0.001$ ; Supporting Fig. 5). TGF- $\beta$ 1 secretion was further quantified in supernatants of mesenchymal 3sp and SNU449 cells by ELISA. In accordance with mRNA levels, Gas6 stimulation caused an increase of TGF- $\beta$ 1 secretion in both cell lines (3sp: 1.6-fold;  $P = 0.006$ ; SNU449: 1.4-fold,  $P = 0.036$ ), which could be reversed by knockdown of Axl or 14-3-3 $\zeta$  (Fig. 5F). Similar results were obtained under unstimulated conditions, showing an autocrine Gas6 feedback loop. These data suggest that Gas6-induced TGF- $\beta$ 1 secretion is mediated by Axl/14-3-3 $\zeta$  signaling.

### Expression of Axl/14-3-3 $\zeta$ in HCC Patients Correlates With Vascular Invasion and Poor Survival

To assess the clinical relevance, levels of Axl, 14-3-3 $\zeta$ , TGF- $\beta$ 1, and phospho-Smad3L were immunohistochemically determined in tumor tissues of HCC patients ( $n = 133$ ). For quantification of expression levels, staining intensities were discriminated (Supporting Fig. 6). Patients expressing high levels of Axl exhibited a more advanced tumor stage ( $P = 0.027$ ) as well as a higher incidence of vascular invasion ( $P < 0.001$ ) and recurrence of disease ( $P = 0.013$ ; Fig. 6A-C; Supporting Table 1). Notably, high Axl levels correlated with poor survival ( $P = 0.005$ ; Fig. 6D). Furthermore, Cox proportional hazard regression revealed association of Axl with poor overall and recurrence-free survival in both uni- and multivariate analysis (Table 1). In addition, we found that the impact of 14-3-3 $\zeta$  levels on the survival of HCC patients was dependent on Axl expression. Levels of 14-3-3 $\zeta$  in HCC patients with low Axl expression did not significantly affect patient survival (data not shown); however, high levels of 14-3-3 $\zeta$  were strongly associated with decreased survival in those patients expressing high Axl ( $P = 0.025$ ; Fig. 6E). These data underline the relevance of 14-3-3 $\zeta$  for Axl-mediated tumor promotion. Neither Axl nor 14-3-3 $\zeta$  levels correlated with clinicopathological parameters, such as age, gender, HCV status, or, most important, cirrhosis (Supporting Tables 1 and 2). However, there was a significant association between high Axl and HBV status. Furthermore, Axl expression strongly correlated with Smad3L-phosphorylation ( $P = 0.0006$ ; Fig. 6F), suggesting that Axl-mediated activation of tumor-promoting Smad3 signaling is crucial in HCC progression. Accordingly, HCC patients exhibiting high phospho-Smad3L levels showed decreased survival, although without statistical significance (Supporting Fig. 7A). No correlation was observed between TGF- $\beta$ 1 expression and Axl or phospho-Smad3L levels (Supporting Fig. 7B). In conclusion, these data indicate that Axl requires 14-3-3 $\zeta$  for the progression of primary human HCC by altering Smad3L phosphorylation.

## Discussion

A central role of Axl has been shown for the development of various types of cancer; however, mechanistic evidence for crucial functions of Axl in HCC progression are very poor. Axl expression was found to be induced by Hippo/YAP signaling and has been correlated with increased up-regulation of Slug and lymphatic metastasis of HCC cells.<sup>16,17,23,24</sup> In this study, we identified the up-regulation and activation of Axl in hepatocellular EMT. Our data suggest that Axl plays a crucial role as a driver of HCC invasion and metastasis. Notably, mass spectrometry analysis of the Axl interactome identified 14-3-3 $\zeta$  as an interaction partner of Axl which has recently been associated with EMT and chemoresistance in HCC.<sup>20,21</sup> The knockdown of 14-3-3 $\zeta$  resulted in the reversion of migratory and invasive responses to Gas6, comparable to the intervention with Axl. As Gas6 exclusively binds to TAM receptors and mesenchymal 3sp cells lack detectable Tyro3 and Mer expression, we conclude that 14-3-3 $\zeta$  is essentially required for Gas6/Axl induced motility of HCC cells.

In HCC, tumor-promoting TGF- $\beta$  signal transduction has been shown to depend on RTK signaling, in particular EGF and HGF/Met. In this context, EGF-R is necessary for AKT activation, which confers resistance to TGF- $\beta$ -mediated apoptosis.<sup>12</sup> With respect to Met, receptor activation leads to phosphorylation of JNK that alters Smad3 phosphorylation and thereby contributes to TGF- $\beta$  resistance.<sup>11</sup> Therefore, we examined a possible crosstalk between Axl and TGF- $\beta$ . Importantly, stimulation of mesenchymal HCC cells with Gas6 increased phosphorylation of Smad3L at Ser213, which has been shown to mediate TGF- $\beta$  resistance and to correlate with metastasis and poor survival in HCC.<sup>25,26</sup> Even though we also observed enhanced phosphorylation of Smad3 at the C-terminal region (Ser425) in response to Gas6, which is described to mediate tumor-suppressive effects, it has been shown that concomitant Smad3L phosphorylation leads to a modified and tumor-promoting Smad3L/C-response.<sup>26,27</sup> Knockdown of Axl or 14-3-3 $\zeta$  abolished these effects on Smad3L phosphorylation. Interestingly, 14-3-3 $\zeta$  has already been associated with resistance to TGF- $\beta$  in murine, Ras-transformed mammary epithelial cells by enhancing phosphorylation of Smad3L region by an unknown mechanism.<sup>28</sup> Our data suggest that this mechanism involves the Gas6/Axl pathway and that Axl requires 14-3-3 $\zeta$  to phosphorylate Smad3 and to switch TGF- $\beta$ -signaling to a pro-oncogenic and TGF- $\beta$  resistant phenotype in HCC.

Axl physically interacts with 14-3-3 $\zeta$ , which is essential for modulation of TGF- $\beta$  signaling. *In silico* analysis revealed that Axl harbors a 14-3-3 binding motif close to its catalytic domain (data not shown). Binding of Axl to 14-3-3 $\zeta$  occurs independently of Gas6 stimulation (Fig. 2B), which opens the issue of how Axl activation transmits its signal by 14-3-3 $\zeta$  to Smad3. Conceivably, 14-3-3 $\zeta$  operates as an adaptor or scaffold protein<sup>29</sup> which mediates Axl activation to downstream signaling effectors. Since Smad3L can be phosphorylated by ERK,<sup>8</sup> which has been shown to be activated by Axl either directly or by PI3K/AKT,<sup>30</sup> we analyzed the activation of MAPK and PI3K by Gas6 in mesenchymal 3sp HCC cells. Although both AKT and PI3K were induced by Gas6, no activation of ERK was observed. It is still possible that PI3K/AKT signaling downstream of Axl contributes to enhanced survival in response to TGF- $\beta$ , albeit through a different mechanism. Importantly, Gas6 caused activation of JNK, a known mediator of Smad3L phosphorylation, and

knockdown of JNK impaired Axl/14-3-3 $\zeta$ -mediated phosphorylation of Smad3L.<sup>31</sup> Thus, Axl/14-3-3 $\zeta$ -mediated phosphorylation of Smad3L is due to activation of JNK. Aberrant SmadL phosphorylation at Ser213 is considered to be responsible for the up-regulation of a TGF- $\beta$ -specific mesenchymal gene expression program. This is underlined by the observation that known tumor-promoting TGF- $\beta$  genes such TGF- $\beta$ 1 itself, PAI1, MMP9, and Snail were increased in mesenchymal HCC cell lines depending on Axl/14-3-3 $\zeta$ . A recent study reported that Axl expression can be induced by TGF- $\beta$  in immune cells.<sup>24</sup> It remains to be investigated whether a similar mechanism acts in HCC as well, leading to an autocrine Axl/TGF- $\beta$  feedback loop. Together, our data suggest that Axl/14-3-3 $\zeta$  signaling is essentially involved in shifting TGF- $\beta$  responses from tumor suppression towards tumor promotion in HCC (Fig. 7).

We further addressed the question whether Axl on its own is a driver of EMT in HCC cells. Neither exogenous expression of Axl caused EMT of epithelial hepatoma cells nor interference with Axl in mesenchymal HCC cells resulted in a complete reversal of EMT by loss of mesenchymal markers (data not shown). However, Axl is crucially required for the maintenance of EMT in HCC due to its role in mediating resistance to TGF- $\beta$ -mediated cell death and due to its impact on TGF- $\beta$  downstream effectors. Similarly, Axl was shown to be essential in EMT of breast cancer.<sup>17</sup>

The clinical relevance of these findings could be demonstrated by analyzing primary tissue samples of HCC patients. Patients expressing high Axl showed more unfavorable disease parameters such as advanced tumor stage, higher incidence of vascular invasion, and tumor recurrence. Additionally, high Axl levels correlated with poor survival of HCC patients. Most interestingly, high levels of Axl associating with strong expression of 14-3-3 $\zeta$  correlated with a tremendous reduction of the median survival of HCC patients from 21.2 to 8.75 months (Fig. 6E). Furthermore, Axl expression strongly correlated with Smad3L phosphorylation, confirming *in vitro* data. These results suggest that modulation of TGF- $\beta$  signaling is crucial for Axl-mediated HCC progression. Thus, Axl/14-3-3 $\zeta$  signaling should be considered a potential therapeutic target to combat HCC progression.

## Supplementary Material

Refer to Web version on PubMed Central for supplementary material.

## Acknowledgments

Supported by the Austrian Science Fund, FWF, P25356; the European Union, FP7 Health Research, HEALTH-F4-2008-202047; the Herzfelder Family Foundation, and People Programme (Marie Curie Actions) of the European Union's Seventh Framework Programme (FP7/2007-2013) under REA grant agreement no. PITN-GA-2012-316549 (IT LIVER).

## Abbreviations

<b>EGF-R</b>	epidermal growth factor receptor
<b>ELISA</b>	enzyme-linked immunosorbent assay



<b>EMT</b>	epithelial to mesenchymal transition
<b>ERK</b>	extracellular signal-regulated kinase
<b>GFP</b>	green fluorescent protein
<b>HBV</b>	hepatitis B virus
<b>HCC</b>	hepatocellular carcinoma
<b>HCV</b>	hepatitis C virus
<b>HSECs</b>	human hepatic sinusoidal endothelial cells
<b>IP</b>	immunoprecipitation
<b>JNK</b>	c-Jun N-terminal kinase
<b>MAPK</b>	mitogen activated protein kinase
<b>MH</b>	mad homology
<b>MMP</b>	matrix metalloproteinase
<b>PAI</b>	plasminogen activator inhibitor
<b>RTK</b>	receptor tyrosine kinase
<b>SmadL</b>	Smad linker
<b>TAM</b>	Tyro3, Axl, Mer
<b>TGF</b>	transforming growth factor
<b>TUNEL</b>	TdT-mediated dUTP-biotin nick end labeling

## References

1. El-Serag HB, Rudolph KL. Hepatocellular carcinoma: epidemiology and molecular carcinogenesis. *Gastroenterology*. 2007; 132:2557–2576. [PubMed: 17570226]
2. Forner A, Llovet JM, Bruix J. Hepatocellular carcinoma. *Lancet*. 2012; 379:1245–1255. [PubMed: 22353262]
3. Reichl P, Haider C, Grubinger M, Mikulits W. TGF-beta in epithelial to mesenchymal transition and metastasis of liver carcinoma. *Curr Pharm Des*. 2012; 18:4135–4147. [PubMed: 22630087]
4. Thiery JP, Acloque H, Huang RY, Nieto MA. Epithelial-mesenchymal transitions in development and disease. *Cell*. 2009; 139:871–890. [PubMed: 19945376]
5. Giannelli G, Villa E, Lahn M. Transforming growth factor-beta as a therapeutic target in hepatocellular carcinoma. *Cancer Res*. 2014; 74:1890–1894. [PubMed: 24638984]
6. Massague J. TGFbeta in cancer. *Cell*. 2008; 134:215–230. [PubMed: 18662538]
7. Heldin CH, Moustakas A. Role of Smads in TGFbeta signaling. *Cell Tissue Res*. 2012; 347:21–36. [PubMed: 21643690]
8. Matsuzaki K. Modulation of TGF-beta signaling during progression of chronic liver diseases. *Front Biosci (Landmark Ed)*. 2009; 14:2923–2934. [PubMed: 19273245]
9. Zulehner G, Mikula M, Schneller D, van Zijl F, Huber H, Sieghart W, et al. Nuclear beta-catenin induces an early liver progenitor phenotype in hepatocellular carcinoma and promotes tumor recurrence. *Am J Pathol*. 2010; 176:472–481. [PubMed: 20008139]
10. Lamouille S, Xu J, Derynck R. Molecular mechanisms of epithelialmesenchymal transition. *Nat Rev Mol Cell Biol*. 2014; 15:178–196. [PubMed: 24556840]

11. Mori S, Matsuzaki K, Yoshida K, Furukawa F, Tahashi Y, Yamagata H, et al. TGF-beta and HGF transmit the signals through JNK-dependent Smad2/3 phosphorylation at the linker regions. *Oncogene*. 2004; 23:7416–7429. [PubMed: 15326485]
12. Murillo MM, del Castillo G, Sanchez A, Fernandez M, Fabregat I. Involvement of EGF receptor and c-Src in the survival signals induced by TGF-beta1 in hepatocytes. *Oncogene*. 2005; 24:4580–4587. [PubMed: 15856020]
13. Lemke G, Rothlin CV. Immunobiology of the TAM receptors. *Nat Rev Immunol*. 2008; 8:327–336. [PubMed: 18421305]
14. Lemke G. Biology of the TAM receptors. *Cold Spring Harb Perspect Biol*. 2013; 5:a009076. [PubMed: 24186067]
15. Tsou AP, Wu KM, Tsen TY, Chi CW, Chiu JH, Lui WY, et al. Parallel hybridization analysis of multiple protein kinase genes: identification of gene expression patterns characteristic of human hepatocellular carcinoma. *Genomics*. 1998; 50:331–340. [PubMed: 9676427]
16. Xu MZ, Chan SW, Liu AM, Wong KF, Fan ST, Chen J, et al. AXL receptor kinase is a mediator of YAP-dependent oncogenic functions in hepatocellular carcinoma. *Oncogene*. 2011; 30:1229–1240. [PubMed: 21076472]
17. Gjerdrum C, Tiron C, Hoiby T, Stefansson I, Haugen H, Sandal T, et al. Axl is an essential epithelial-to-mesenchymal transition-induced regulator of breast cancer metastasis and patient survival. *Proc Natl Acad Sci U S A*. 2010; 107:1124–1129. [PubMed: 20080645]
18. Zhang YX, Knyazev PG, Cheburkin YV, Sharma K, Knyazev YP, Orfi L, Szabadkai I, et al. AXL is a potential target for therapeutic intervention in breast cancer progression. *Cancer Res*. 2008; 68:1905–1915. [PubMed: 18339872]
19. Aitken A. Post-translational modification of 14-3-3 isoforms and regulation of cellular function. *Semin Cell Dev Biol*. 2011; 22:673–680. [PubMed: 21864699]
20. Choi JE, Hur W, Jung CK, Piao LS, Lyoo K, Hong SW, et al. Silencing of 14-3-3zeta over-expression in hepatocellular carcinoma inhibits tumor growth and enhances chemosensitivity to cis-diammined dichloridoplatinum. *Cancer Lett*. 2011; 303:99–107. [PubMed: 21334806]
21. Huang XY, Ke AW, Shi GM, Zhang X, Zhang C, Shi YH, et al. alphaB-crystallin complexes with 14-3-3zeta to induce epithelialmesenchymal transition and resistance to sorafenib in hepatocellular carcinoma. *Hepatology*. 2013; 57:2235–2247. [PubMed: 23316005]
22. van Zijl F, Mall S, Machat G, Pirker C, Zeillinger R, Weinhaeusel A, et al. A human model of epithelial to mesenchymal transition to monitor drug efficacy in hepatocellular carcinoma progression. *Mol Cancer Ther*. 2011; 10:850–860. [PubMed: 21364009]
23. Lee HJ, Jeng YM, Chen YL, Chung L, Yuan RH. Gas6/Axl pathway promotes tumor invasion through the transcriptional activation of Slug in hepatocellular carcinoma. *Carcinogenesis*. 2014; 35:769–775. [PubMed: 24233839]
24. Bauer T, Zagorska A, Jurkin J, Yasmin N, Koffel R, Richter S, et al. Identification of Axl as a downstream effector of TGF-beta1 during Langerhans cell differentiation and epidermal homeostasis. *J Exp Med*. 2012; 209:2033–2047. [PubMed: 23071254]
25. Kim SH, Ahn S, Park CK. Smad3 and its phosphoisoforms are prognostic predictors of hepatocellular carcinoma after curative hepatectomy. *Hepatobil Pancreat Dis Int*. 2012; 11:51–59.
26. Matsuzaki K. Smad phosphoisoform signaling specificity: the right place at the right time. *Carcinogenesis*. 2011; 32:1578–1588. [PubMed: 21798854]
27. Tarasewicz E, Jeruss JS. Phospho-specific Smad3 signaling: impact on breast oncogenesis. *Cell Cycle*. 2012; 11:2443–2451. [PubMed: 22659843]
28. Hong HY, Jeon WK, Bae EJ, Kim ST, Lee HJ, Kim SJ, et al. 14-3-3 sigma and 14-3-3 zeta plays an opposite role in cell growth inhibition mediated by transforming growth factor-beta 1. *Mol Cells*. 2010; 29:305–309. [PubMed: 20082218]
29. Obsil T, Obsilova V. Structural basis of 14-3-3 protein functions. *Semin Cell Dev Biol*. 2011; 22:663–672. [PubMed: 21920446]
30. Korshunov VA. Axl-dependent signalling: a clinical update. *Clin Sci (Lond)*. 2012; 122:361–368. [PubMed: 22187964]

31. Matsuzaki K, Seki T, Okazaki K. TGF-beta signal shifting between tumor suppression and fibro-carcinogenesis in human chronic liver diseases. *J Gastroenterol.* 2014; 49:971–981. [PubMed: 24263677]

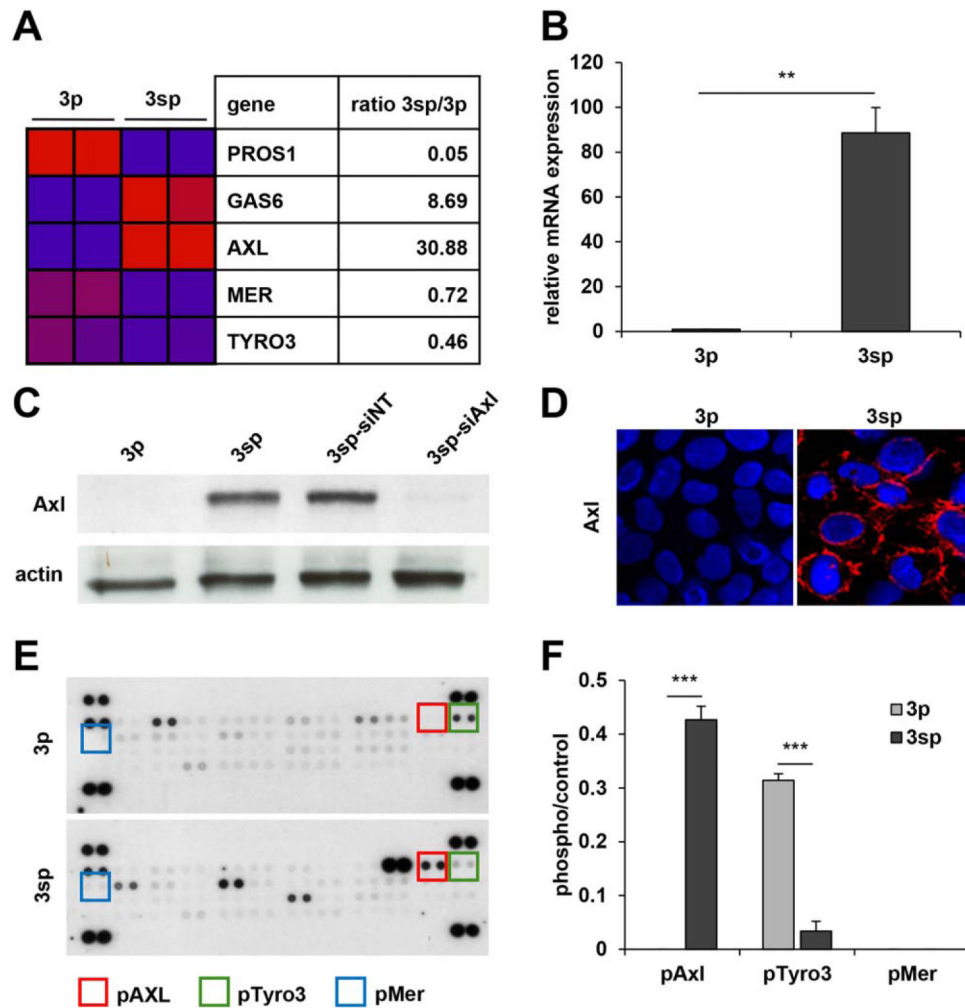


**Fig. 1.** Expression of TAM receptors and their ligands in epithelial and mesenchymal HCC cells. (A) Down-regulation (blue) and up-regulation (red) of Tyro3, Axl, Mer, and their ligands Gas6 and Protein S (PROS1) in epithelial 3p and mesenchymal 3sp cells as assessed by whole-genome expression analysis. (B) Axl mRNA levels in 3p and 3sp cells analyzed by qRT-PCR. (C) Western blot analysis of Axl expression in 3p and 3sp cells. Actin was used as loading control. (D) Localization of Axl as shown by confocal immunofluorescence analysis (red). (E) Phospho-RTK array analysis of 3p and 3sp cells. Rectangles indicate phosphorylation of TAM receptors. (F) Quantification of TAM phosphorylation in 3p and 3sp cells. Data are expressed as mean  $\pm$  SD. \*\* $P < 0.01$ ; \*\*\* $P < 0.001$ .

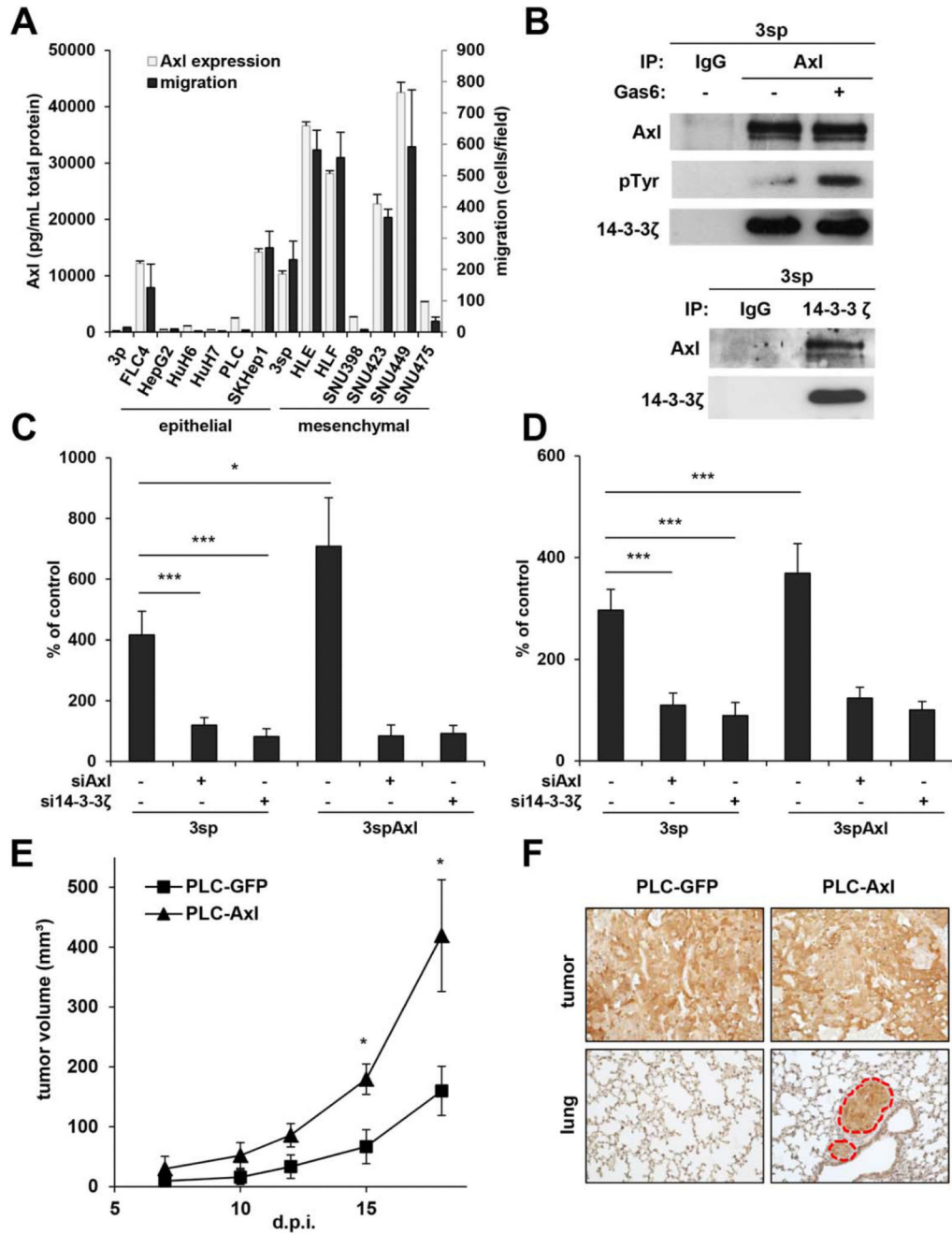


**Fig. 2.** Role of Axl and 14-3-3ζ in migration, transendothelial invasion, and metastasis of HCC cells. (A) Fourteen hepatoma cell lines were analyzed for Axl expression by ELISA and migration. (B) Immunoprecipitation against Axl with and without Gas6 stimulation (500 ng/mL; upper panel). Phosphorylation of Axl by Gas6 and interaction with 14-3-3ζ as shown by immunoblotting against phosphotyrosine and 14-3-3ζ. Lower panel: Immunoprecipitation of 14-3-3ζ and probing for Axl. (C) Transwell migration of 3sp and Axl-overexpressing 3spAxl cells after stimulation with Gas6 (500 ng/mL) and interference with Axl or 14-3-3ζ

by siRNA. (D) Transendothelial invasion of 3sp and 3spAxl cells through a monolayer of HSECs after incubation with Gas6 (500 ng/mL) and interference with Axl or 14-3-3 $\zeta$  by siRNA. Data are expressed as mean  $\pm$  SD. (E) Tumor growth of Axl-overexpressing PLC/PRF/5 cells (PLC-Axl; n = 4), injected subcutaneously into NSG mice, as compared to control (PLC-GFP; n = 4). (F) Immunohistochemical analysis of GFP in primary subcutaneous tumors and lung metastasis 30 days postresection of subcutaneous tumors derived from PLC-GFP (n = 4) and PLC-Axl (n = 4). Red broken circles indicate metastatic nodules. Data are expressed as mean  $\pm$  SEM. d.p.i., days postinjection; NT, nontarget. \* $P$  < 0.05; \*\*\* $P$  < 0.001.

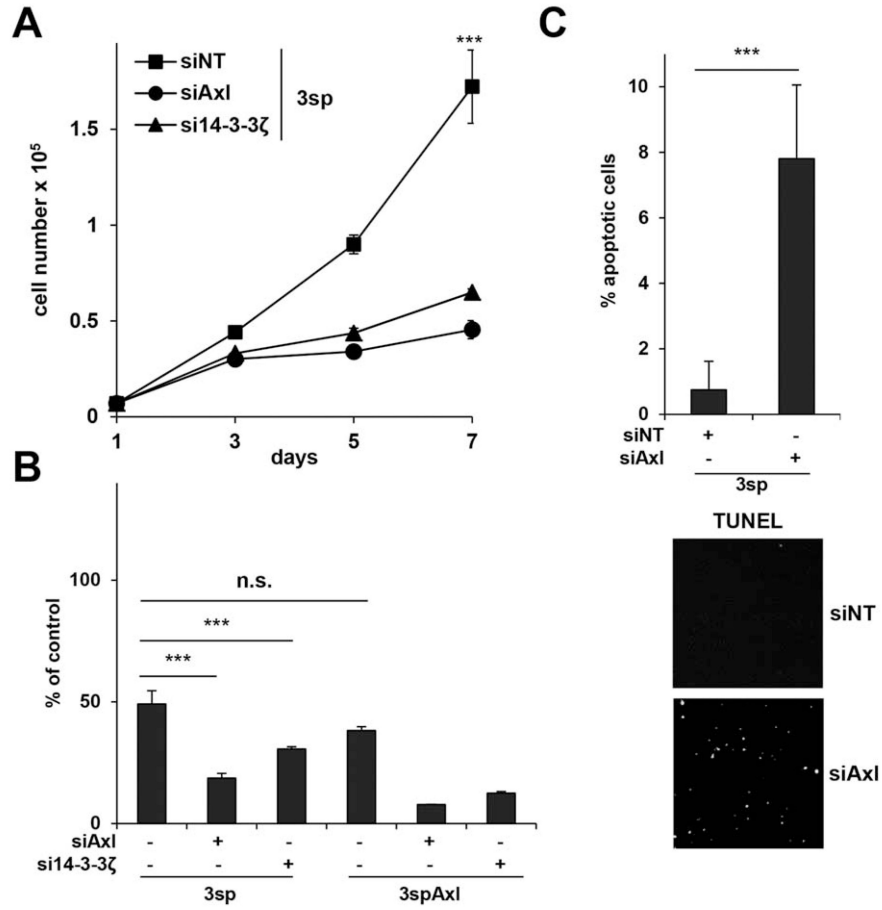


**Fig. 3.** Role of Axl and 14-3-3 $\zeta$  in TGF- $\beta$  resistance. (A) Proliferation kinetics of 3sp cells incubated with TGF- $\beta$ 1 (2.5 ng/mL) after knockdown of Axl or 14-3-3 $\zeta$ . (B) Cell survival of 3sp and 3spAxl cells after treatment with TGF- $\beta$ 1 (2.5 ng/mL) for 7 days and interference with Axl or 14-3-3 $\zeta$ . (C) Induction of cell death by TGF- $\beta$ 1 in 3sp cells after knockdown of Axl as shown by TUNEL assay. Cells were treated with 10 ng/mL TGF- $\beta$ 1 for 24 hours. Lower panel shows images of TUNEL-positive cells by fluorescence microscopy. Data are expressed as mean  $\pm$  SD. \*\*\* $P < 0.001$ ; n.s., nonsignificant.

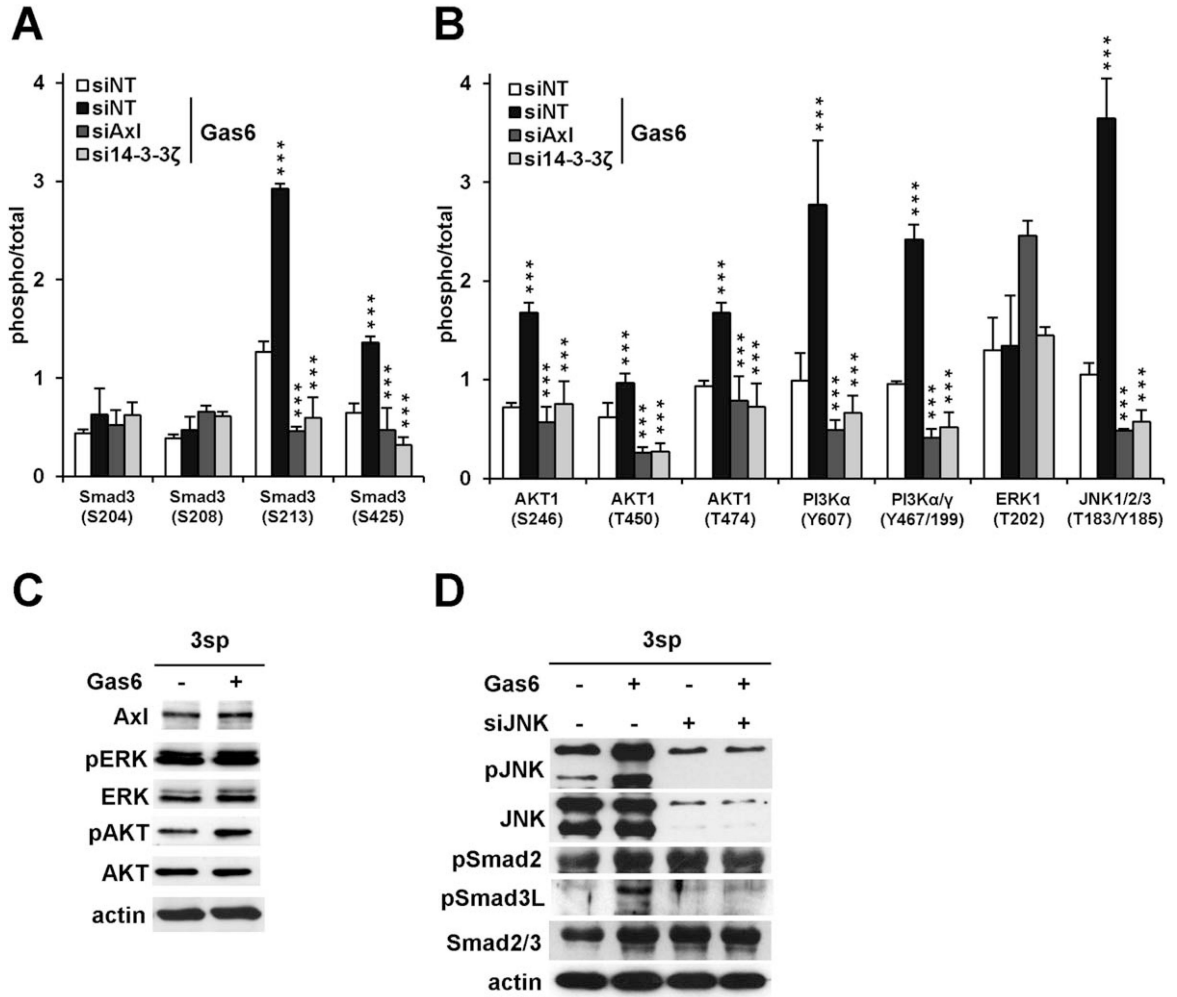


**Fig. 4.** Modulation of TGF- $\beta$  signaling by the Gas6/Axl/14-3-3 $\zeta$  axis. (A) Phosphorylation of Smad3 was assessed by phospho-specific antibody microarrays in untreated 3sp control cells (siNT) and 3sp cells with a knockdown of Axl or 14-3-3 $\zeta$  (siAxl, si14-3-3 $\zeta$ ). Cells were treated with Gas6 (500 ng/mL) for 15 minutes or left untreated (siNT). (B) Phosphorylation of PI3K/AKT, ERK, and JNK by Gas6 in 3sp cells with and without interference with Axl or 14-3-3 $\zeta$  as detected by array analysis. (C) Western blot analysis of ERK and AKT in 3sp cells with and without Gas6 stimulation (500 ng/mL). Actin was used as loading control. (D) Western blot analysis of JNK, phospho-Smad2 (pSmad2), phospho-Smad3L (pSmad3L), and total Smad2/3 after stimulation with Gas6 (500 ng/mL) and interference with JNK by siRNA (siJNK). Data are expressed as mean  $\pm$  SD. \*\*\* $P$  < 0.001.



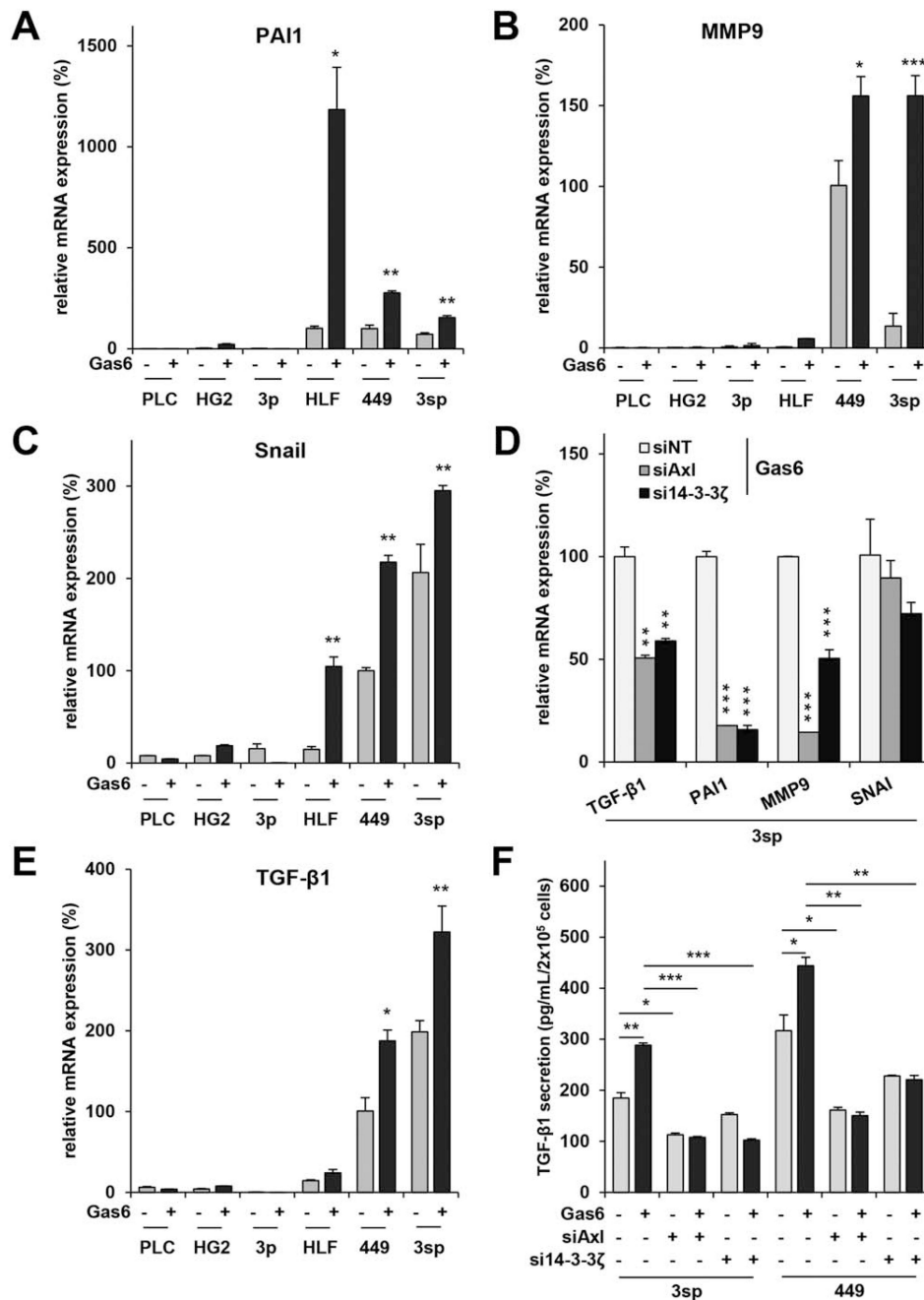


**Fig. 5.** Axl/14-3-3 $\zeta$  activates tumor-promoting TGF- $\beta$  target genes and autocrine TGF- $\beta$  signaling. qRT-PCR analysis of epithelial PLC/PRF/5 (PLC), HepG2 (HG2), and 3p HCC cells as well as mesenchymal HLF, SNU449 (449), and 3sp cells after stimulation with Gas6 for 8 hours. (A-C) Analysis of PAI1, MMP9, and Snail. Untreated SNU449 were 100%. (D) Repression of TGF- $\beta$  target gene expression in 3sp cells after stimulation with Gas6 (500 ng/mL) for 8 hours and knockdown of Axl or 14-3-3 $\zeta$ . (E) Analysis of TGF- $\beta$ 1 mRNA expression. (F) Secretion of TGF- $\beta$ 1 protein was analyzed by ELISA in supernatants of 3sp and SNU449

cells with or without a knockdown of Axl or 14-3-3 $\zeta$ . Cells were untreated or treated with 500 ng/mL Gas6 for 24 hours. Data are expressed as mean  $\pm$  SD. \* $P$  < 0.05; \*\* $P$  < 0.01; \*\*\* $P$  < 0.001.

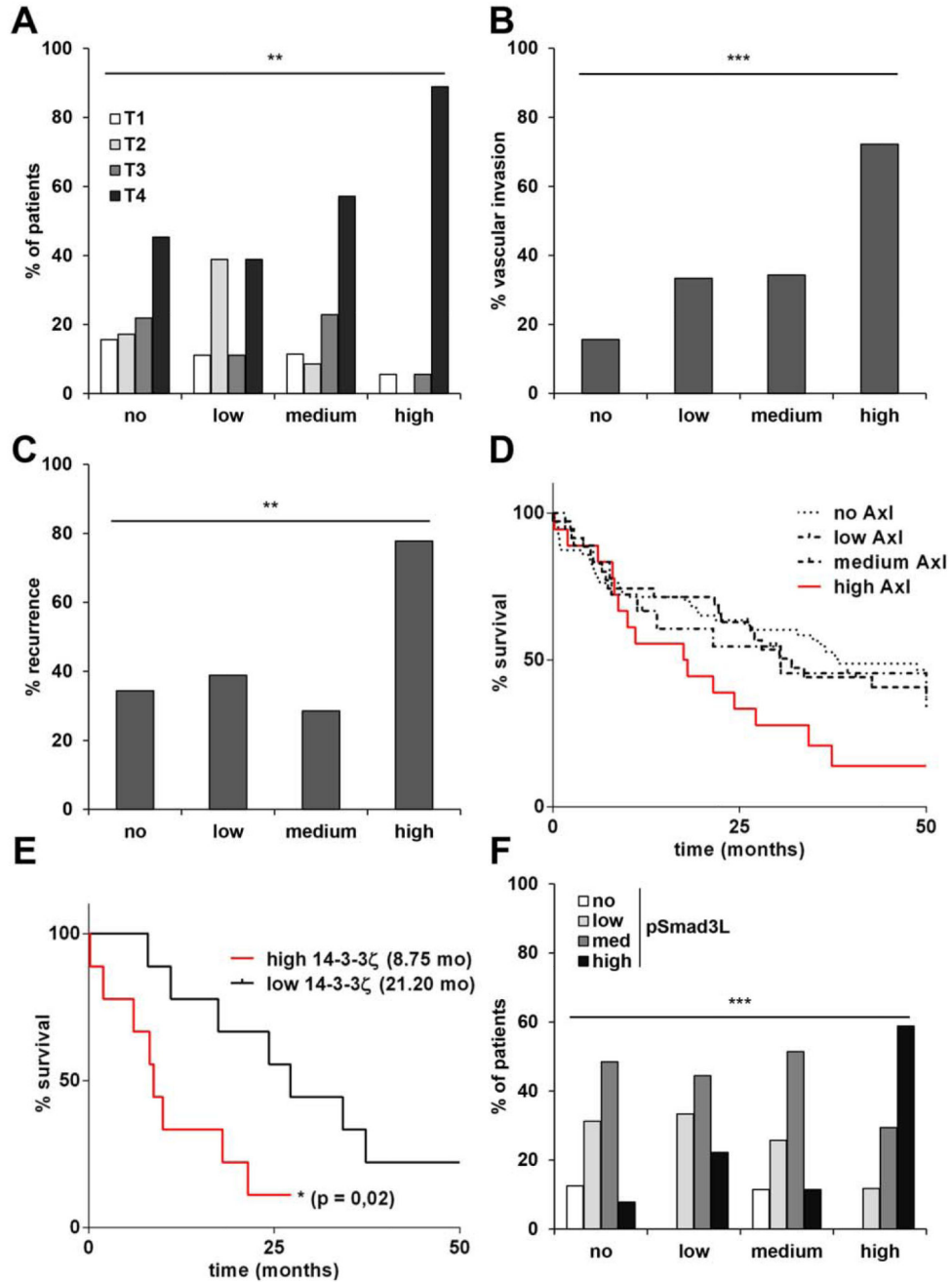


**Fig. 6.** Correlation of Axl and 14-3-3 $\zeta$  levels with prognosis and survival of HCC patients. Immunohistochemical staining intensities of Axl were scored with no, low, medium, and high protein levels. (A) Correlation of staining intensities with tumor stages, (B) vascular invasion, (C) recurrence of disease. (D) Kaplan-Meier survival analysis of patients. (E) Kaplan-Meier survival analysis of patients expressing high Axl and either low or high 14-3-3 $\zeta$ . (F) Correlation of Axl expression with phospho-Smad3L (pSmad3L) levels. Numbers in parentheses indicate median survival in months. \*\* $P < 0.01$ ; \*\*\* $P < 0.001$ .

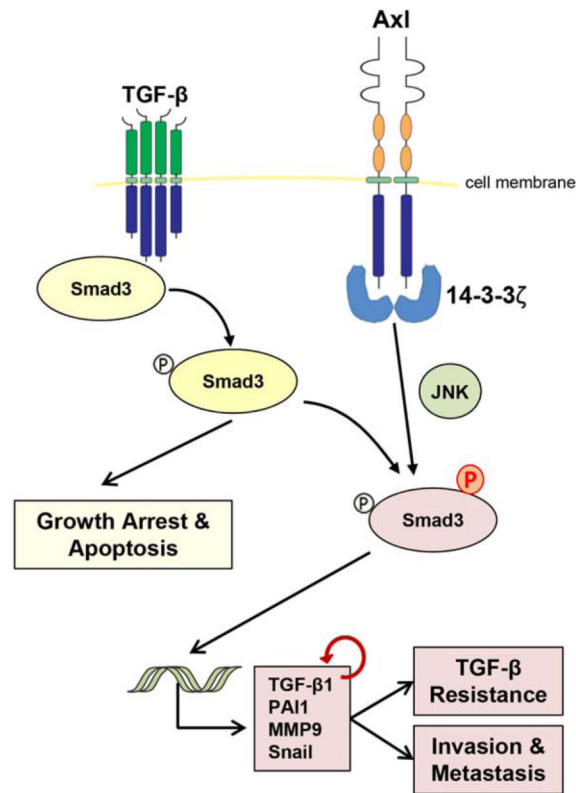


**Fig. 7.** Scheme depicting the molecular cooperation between Axl/14-3-3 $\zeta$  and TGF- $\beta$  signaling. Phosphorylation of Smad3L by Axl/14-3-3 $\zeta$  and JNK induces the expression of tumor-progressive TGF- $\beta$  target genes leading to autocrine TGF- $\beta$ 1 activation (circled arrow) and invasion of HCC by escape from TGF- $\beta$  sensitivity.

**Table 1**  
**Univariate and multivariate survival analysis by Cox proportional hazard regression**

Variable	Overall survival			Recurrence-free survival		
	HR	CI 95 %	P	HR	CI 95 %	P
<i>univariate analysis</i>						
Age	0.967	0.943-0.993	0.012**	0.977	0.954-1.001	0.062
Gender	1.797	0.717-4.506	0.211	1.456	0.663-3.197	0.349
HBV status	1.220	0.552-2.695	0.623	1.235	0.587-2.599	0.579
HCV status	0.519	0.274-0.981	0.043**	0.567	0.313-1.026	0.061
Cirrhosis	0.496	0.257-0.959	0.037**	0.471	0.255-0.869	0.016**
TNM stage	1.842	1.488-2.280	0.000*	1.836	1.503-2.243	0.000*
AxI	3.640	1.906-6.950	0.000*	4.007	2.137-7.514	0.000*
<i>multivariate analysis</i>						
Age	0.970	0.939-1.001	0.058	0.991	0.962-1.022	0.568
Gender	1.128	0.355-3.590	0.838	1.255	0.454-3.465	0.662
HBV status	0.475	0.176-1.282	0.142	0.684	0.279-1.681	0.408
HCV status	0.531	0.254-1.111	0.093	0.725	0.360-1.461	0.369
Cirrhosis	1.249	0.511-3.053	0.626	0.859	0.380-1.943	0.716
TNM stage	1.919	1.482-2.486	0.000*	1.746	1.395-2.186	0.000*
AxI	2.053	1.026-4.108	0.042**	2.218	1.135-4.332	0.020**

CI, confidence interval. HR, hazard ratio. HBV, hepatitis B virus. HCV, hepatitis C virus.

\*  $P < 0.001$ .

\*\*  $P < 0.05$ .